International Conference on Space Optics—ICSO 2010

Rhodes Island, Greece

4–8 October 2010

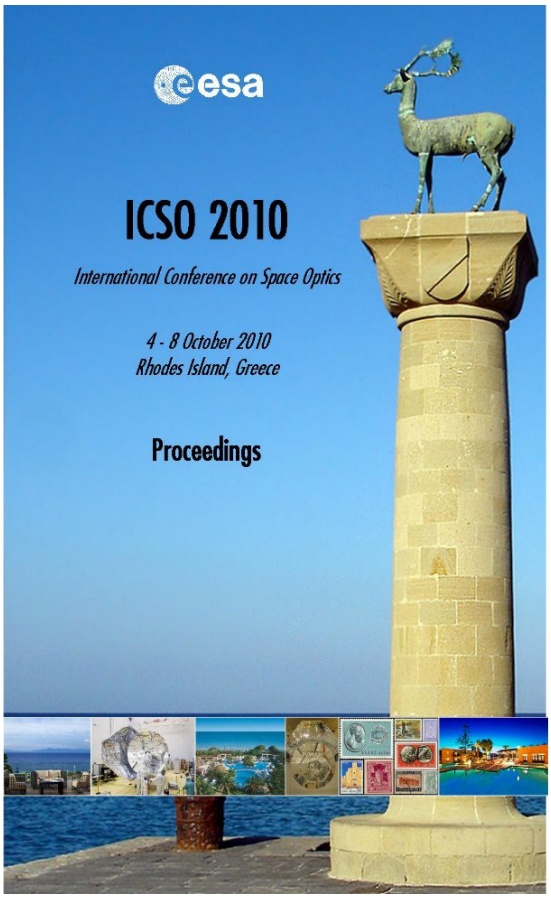

Edited by Errico Armandillo, Bruno Cugny, and Nikos Karafolas

Imaging lidar technology: development of a 3D-lidar elegant breadboard for rendezvous and docking, test results, and prospect to future sensor application

B. Moebius, M. Pfennigbauer, J. Pereira do Carmo

esa icso proceedings cnes

International Conference on Space Optics — ICSO 2010, edited by Errico Armandillo, Bruno Cugny, Nikos Karafolas, Proc. of SPIE Vol. 10565, 105650H · © 2010 ESA and CNES
CCC code: 0277-786X/17/$18 · doi: 10.1117/12.2309246

IMAGING LIDAR TECHNOLOGY - DEVELOPMENT OF A 3D-LIDAR ELEGANT BREADBOARD FOR RENDEZVOUS AND DOCKING, TEST RESULTS, AND PROSPECT TO FUTURE SENSOR APPLICATION

B. Moebius[1], M. Pfennigbauer[2], J. Pereira do Carmo[3]
[1]Jena-Optronik, Pruessingstr. 41, 07745 Jena, Germany; [2]Riegl Measurement Systems, Riedenburgstr. 48, 3580 Horn, Austria; [3]ESTEC, Keplerlaan 1, 2200 AG Noordwijk zh, The Netherlands

I. INTRODUCTION

Keywords: Rendezvous and Docking Sensor, RVS, 3D LIDAR, Imaging LIDAR

During the previous 15 years, Rendezvous and Docking Sensors (RVS) were developed, manufactured and qualified. In the mean time they were successfully applied in some space missions: For automatic docking of the European ATV "Jules Verne" on the International Space Station in 2008; for automatic berthing of the first Japanese HTV in 2009, and even the precursor model ARP-RVS for measurements during Shuttle Atlantis flights STS-84 and STS-86 to the MIR station. Up to now, about twenty RVS Flight Models for application on ATV, HTV and the American Cygnus Spacecraft were manufactured and delivered to the respective customers.

RVS is designed for tracking of customer specific, cooperative targets (i.e. retro reflectors that are arranged in specific geometries). Once RVS has acquired the target, the sensor measures the distance to the target by time-of-flight determination of a pulsed laser beam. Any echo return provokes an interrupt signal and thus the readout of the according encoder positions of the two scan mirrors that represent Azimuth and Elevation measurement direction to the target. [2], [3].

The capability of the RVS for 3D mapping of the scene makes the fully space qualified RVS to be real 3D Lidar sensors; thus they are a sound technical base for the compact 3D Lidar breadboard that was developed in the course of the Imaging Lidar Technology (ILT) project.

II. IMAGING LIDAR FOR ESA EXPLORATION MISSIONS

A. Aim of the 3D Lidar Development

Development of the 3D Lidar in the ILT project was founded by the European Space Agency (ESA) in the frame of the Technology and Research Programme, and aiming future exploration missions, like the ones foreseen on the Aurora Programme. The first Flagship missions in the Aurora program are ExoMars and Mars Sample Return. From the requirements of these undertakings three major potential applications for Imaging Lidars sensors can be derived: A Landing Lidar for support of the Guidance, Navigation and Control(GN&C) functions and in particular for selection of a safe landing site; a 3D Lidar providing inputs to Rover navigation and as a substitution or complement to the usual stereo camera on the Rover head by an actively distance measuring 3D sensor; a Rendezvous and Docking sensor to provide the inputs to GN&C during final approach of the sample return canister to the mother spacecraft in the Mars orbit [1].

Each of these sensors shall be small and lightweight, with low power consumption. Since 3D Lidar sensors covering all needs of application during their missions to, on and around Mars are not available off-the-shelf, technology development is required. Application of the new technologies for more than one of the 3D Lidars in the Aurora project would be of benefit at least concerning cost and development time.

In general, the 3D Lidars can be classified into "large-sized" and "small-sized" Lidars, depending on their specific application and resulting specification. Small-sized 3D Lidars are applicable for measurement of cooperative targets at short and long distance (up to a few hundred or thousand meters) and of non-cooperative surfaces at short distance. Large-sized 3D Lidars are applicable for measurements of non-cooperative objects at short and long distance. The wording "small-sized" and "large-sized" are also related with some specifications of the Lidar sensor: A scanning Lidar that transmits a collimated beam, requires comparatively high transmitted laser power and large aperture of the receiver telescope for 3D Lidar application on non-cooperative targets at long range. The 3D Lidar classification into a small-sized and a large-sized type also indicates that – up to a point – utilization of the same or a similar technology is applicable in graded dimension for Lidar type and usage.

B. Requirements to the 3D Lidar for the Mars Sample Return mission

The technical requirements on the 3D Lidar sensor for future application in the Mars Sample Return mission are derived from the need of acquisition and tracking of a small target sphere that is equipped with corner cubes,

i.e. representing a cooperative target. According to the classification above, a small-size Lidar type results, but the technologies of this sensor can also be applicable for corresponding large-size 3D Lidar sensors, as it will be shown in this publication.

The development status of the current sensor RVS ILT is those of an Elegant Breadboard (BB). The sensor consists of a combination of specific components that were developed in the Imaging Lidar Technology project, and off-the-shelf components with no or minor technology relevance.

Table 1 summarizes major requirements of the ILT RVS. The requirements for mass and power consumption are related to a future flight model (FM), but the design of the technology relevant components in the BB gives an indication of the according future sensor properties just now. The required measurement accuracy is related to the determination of the target sphere position. In paragraph "D. Test and Test Results" both the measured accuracy of the target sphere position and those of the single spot measurement during 3D scanning will be discussed.

Table 1. Main performance requirements of the ILT RVS

Parameter	Requirement
Field of view (FOV)	>= 20° x 20°
Frame rate in Track Mode	>= 1 Hz
Acquisition duration	<= 1 min
Min. operational Range (R)	<=1m
Max. operational Range (R)	>=5000m
Measurement accuracy 3σ	R=5000m: ± 1 m R=1m: ± 2 cm
Angular measurement accuracy 3σ	<= 0.2 deg
Sensor mass (requirement / goal)	10 kg / 7 kg
Power consumption (req. / goal)	50 W / 30 W

Fig. 1a) contains a photo of the target sphere for test purposes. Its design is derived from those of the future mars sample return application, but reduced to the necessary optical features. During the mission, the target canister will be tumbling. Therefore, measures for its successful track independent on the rotation stage of the canister are required even in the optical design of the tests target sphere.

The sphere has a diameter of 20 cm and is equipped with 12 arrays of retro reflectors (RR). The RR arrays consist of 6 single corner cubes of 12 mm diameter each that are arranged in such a relative angle to each other that the echo power variation over the sphere is minimum during tumbling. During the optimization process the specified limitations of array area and depth, and the general design of the original canister were considered.

Simulations led to an optimum relative angle of the retro reflectors within one array of 25 deg each.

Fig. 1b) visualizes the solution.

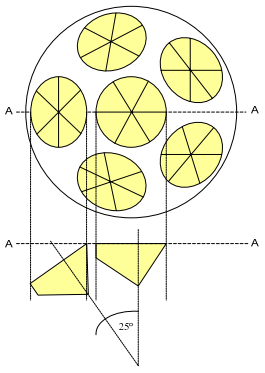

Fig. 1a) Test target sphere containing 12 RR arrays **b)** Geometry of 1 of the retro reflector arrays

C. RVS ILT – Major Design Features

Sensor principle

In Fig. 2 the 3D Lidar sensor principle is visualized. A pulsed Laser beam is transmitted from the Laser range finder (LRF) via fibre cable and optical frontend to the Gimbal mounted scan mirror in the sensor head. The scan mirror deflects the beam to the target. Depending on target type – non-cooperative or cooperative – an echo beam is back scattered or back reflected to the sensor head and – via optical frontend and receiver fibre cable – redirected to the LRF. The Processor Unit (PU) in co-operation with the scanner electronics provides the scanner control and processes the data including correct assignment of range and angles.

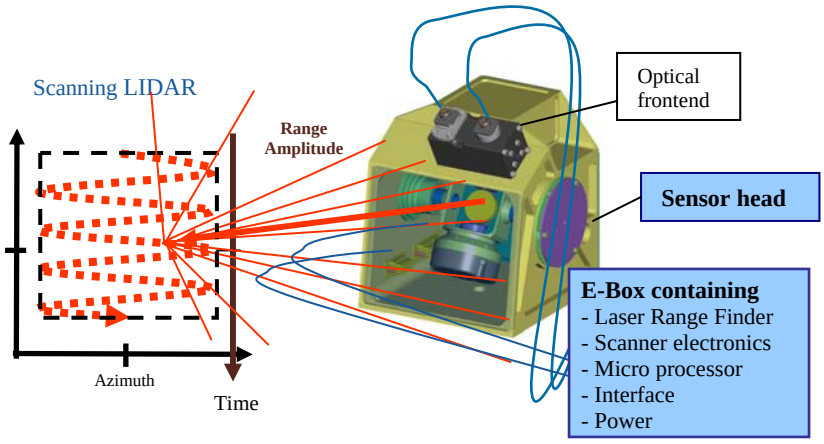

Fig. 2. RVS ILT sensor principle

Sensor head:

Fig. 3a) shows a photo of the fully equipped compact sensor head (150 x 160 x 130 mm³, 1.6 kg, both including LRF frontend). It contains the Gimbal mounted scan mirror with the according motors and encoders for elevation (horizontal, fixed axis) and azimuth driving and control. In zero-zero direction the transmitted beam is directed horizontally for nominal sensor head accommodation. An all-side metalized alignment cube was positioned inside the sensor head. According drilling holes in the sensor head body allow for multi-directional usage of the alignment cube with external autocollimator telescopes.

The current application of a Gimbal mounted scan mirror, compared with the separated azimuth and elevation mirrors as in the former RVS design, leads to a significantly smaller sensor head, and to flexibility in the definition of sensor field-of view. The size of the optical head is now mainly driven by the size of drivers and encoders on the scan axes. The required mirror size slightly exceeds the aperture of the receiver telescope only, provided that a coaxial optics design for the transmitter and receiver beam is selected.

Fig. 3b) and paragraph 'Laser Range Finder' provide details of the optics solution in the LRF optical frontend.

A further design artifice apart of the coaxial beams allows taking full advantage of the Gimbal mounted mirror solution: The intersection of the mutual perpendicular azimuth and elevation axes is positioned in the centre of the scan mirror surface by mirror fixation on a cranked azimuth shaft. As a result, data correction during their processing can be reduced to a minimum in the sensor software (SW). In addition, the mechanical-optical adjustment effort and the calibration effort of the sensor can be minimized by application of low-tolerance design and component manufacturing.

Laser range finder (LRF):

Fig. 3b) shows the LRF coaxial optical frontend that consists of laser collimating optics with a limiting aperture of 2.5 mm diameter, the receiver optics coupling to an FC fibre port, a beam folding mirror, and the receiver mirror with a centre hole for the transmitter beam to pass through. All components are combined in a stable, compact, and lightweight mechanical structure of 66 x 45 x 30 mm³ volume and 150 g total mass.

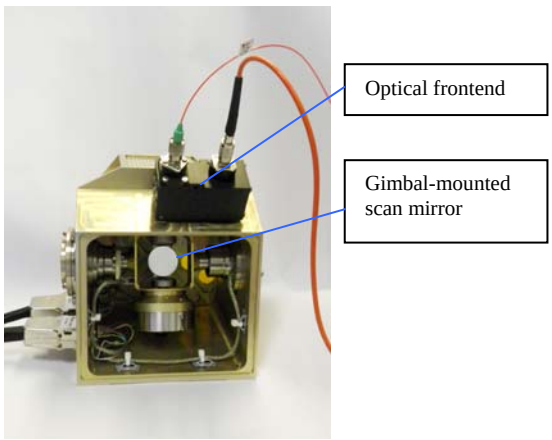

Fig. 3a) RVS ILT sensor head

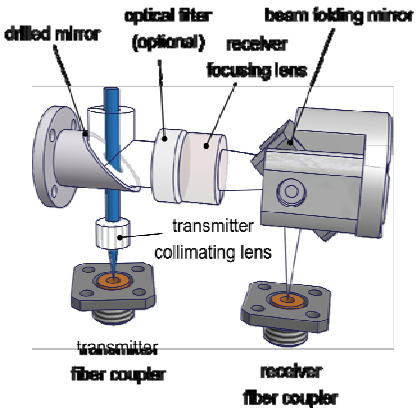

b) 3D view of the optical front-end

The LRF is based on pulsed time-of-flight (TOF) measurement with echo digitization and online waveform processing. A fibre laser is employed for several reasons: high beam quality, scalability of output power, flexibility with respect to pulse duration and pulse repetition rate, compact size, and fair efficiency. The fibre laser used for the sensor has a mean output power of about 50 mW and is operated at a pulse repetition rate of 30 kHz, allowing for an unambiguity range of more than 5 km. For applications where it is necessary to measure to diffusely reflecting targets at long range, the average output power can be increased by a factor of 20 to about 1 W without changing the form factor.

The duration of the laser pulses is a few nanoseconds in order to have high spatial resolution and high precision (repeatability). The receiver frontend comprises an Avalanche Photo Diode (APD) with 200 µm diameter accompanied by a transimpedance amplifier matched for the signal bandwidth and designed to have a high dynamic range. The echo signals are digitized with a sampling rate matched to the pulse duration.

The TOF of the echo signal (calculation in real time) is determined by online waveform processing of the target returns and reference pulses generated with each laser shot. The range to the target (i.e. the target corresponding to the individual laser shot) is calculated from the laser pulse time of flight.

The range values, delivered over Ethernet together with the calibrated optical amplitude, are time-stamped with an internal clock. [4], [5], [6].

Sensor driving, data processing and output:

RVS ILT works on different modes. When applied as a real 3D imager, a data stream output containing range, azimuth, elevation, echo amplitude and time values for each echo return, is transmitted via Ethernet LAN interface. This sensor mode is applicable for client inspection or for 3D scanning of surface at short range. With the envisaged increased Laser power output and/or a larger aperture on receiver side 3D scanning a distance in the order of kilometres will be feasible.

When the sensor is applied for rendezvous and docking purposes, the data output (also via Ethernet LAN interface) provides the position of the target sphere centre with 1 Hz update rate, after according internal processing of the 3D echo data received from the surface of the client. Knowledge of the target sphere geometry and its optical properties is applied in the processing SW for correct centre determination from the surface data.

In both applications of the RVS ILT – as a 3D imager, or for rendezvous with a target sphere – the actually applied FOV can be modified, and its position inside the total FOV can be varied with the actual need. The smaller scan window (down to about 1° x 1°) allows increase of the image update rate or of the measurement point density.

Currently the azimuth and elevation axes of the scan mirror are driven in sine scans (progressive mode). Due to the selected scanner control method, different customer specific scan pattern over the scene can be defined.

The LRF can be operated with different Laser output power depending on type and distance of the target. This feature is really necessary in view of the echo return power that may vary in the order of 10^6 or more, in particular for track of retro reflector targets over kilometres. The default output power is defined at lowest level for protection of the APD in the LRF receiver channel, and is changeable by command.

D. Tests and Test Results on the 3D Lidar RVS ILT

Several functional and performance tests were performed after sensor manufacturing and commissioning.

The most interesting tests and their results shall be introduced here.

RVS ILT as a 3D imager

Fig. 4 shows the 3D image of the test target sphere. The different colours represent the different range to the actually hit retro reflector in the spherical surface. The weaker the echo signal the less saturated is the colour. Therefore, the weak return from the apex of the sphere that is visible in the data stream and can be visualized in the figure just by extreme magnification of the image.

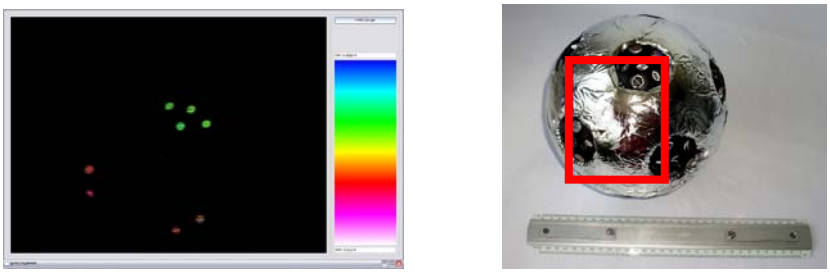

Fig. 4 Test sample and test result for 3D measurement of a cooperative target

Fig. 5 shows 3D imaging of a diffusely reflecting structure (top left), provided by DLR Bremen.

The 3D visualization from scanning the structure is visible on top right side. Diagrams of the cut through the 3D image are visible on lower part of the figure. They were generated on 1½ scan out of the total 3D image each. Resolution of the structure by RVS ILT 3D-imaging worked properly, down to about 1.5 mm. No obvious difference in resolution of grey silk finished (left) and red machine finished surfaces (right side) was identified.

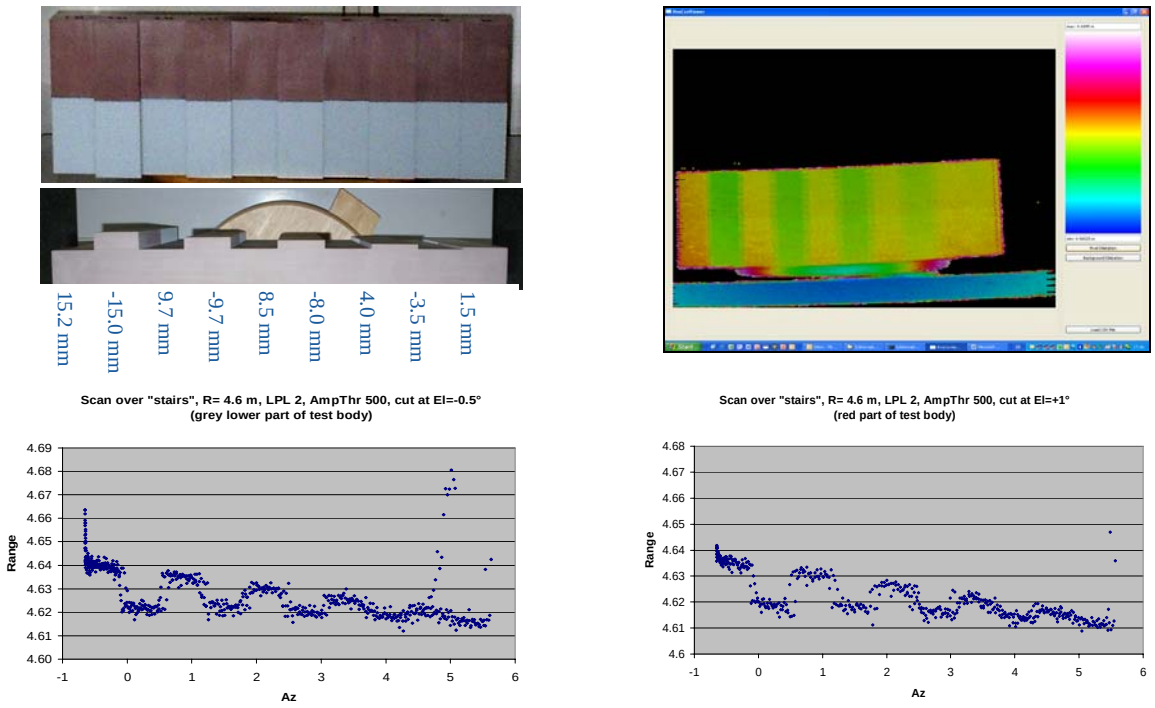

Fig. 5 **Test sample and test result for 3D measurement of a non-cooperative target**

RVS ILT for target acquisition and track

Short-range test for verification of the measurement accuracy with the specific target under rotation conditions (simulating later tumbling of the canister in space) were performed between R = 1 m and R = 20 m. The measured 3 σ range noise was < ± 1 cm even with the tumbling sphere. As a result of the tests, range correction of 7.5 cm independent on range must be applied for calculation of sphere centre from the surface values.

The (seeming) 3 σ azimuth and elevation noise of the tumbling sphere is increasing at very short range and is > ± 0.2 deg specification for R < 3 m. Obviously, the combination of large angular size of the sphere and different distribution of the corner cube with the rotation lead to different "angular scenarios" as long as no specific, target geometry based corrections are implemented in the SW. During some of the test, data "vanished" during processing in the sensor due to problems with the small but rather inefficient processor unit (PU). These effects probably have provoked worse test results than achievable with a faultless PU in some cases. Apart of all endeavour made, the PU problem was not solved in the frame of the project, but shall be overcome by application of a more powerful PU in an ongoing sensor upgrade now.

Dynamic long-range checks were performed over 250 m in the Ribatejo plain (Portugal) with excellent performance results, but under harsh environmental conditions (dust, temperature) leading to sensor break-down at the end. After sensor repair, the remaining maximum range test was performed over a valley under static conditions, over a range of 4750 m. Table 2 summarizes the main test results. The range specific limits for the total error (i.e. bias + noise) are listed under "Requ.", the 3σ noise measurement results under "Meas." Except for Azimuth and Elevation at very short range, there is sufficient margin for the sensor bias.

Increasing angular and range noise at very long range results from atmospheric disturbances. Thus it is expected to be smaller under space conditions.

Table 2 Compilation of the major RVS ILT test results during track

Range [m]	Target / Rotating?	Range 3σ noise [m]		Az 3σ noise [deg]		El 3σ noise [deg]	
		Requ.	Meas.	Requ.	Meas.	Requ.	Meas.
1	Sphere, rotation	± 0.020	± 0.009	± 0.2	± 0.72	± 0.2	± 0.53
8	Sphere, rotation	± 0.036	± 0.006	± 0.2	± 0.091	± 0.2	± 0.076
30	Sphere, rotation	± 0.049	± 0.005	± 0.2	± 0.025	± 0.2	± 0.025
120	Sphere, no rotation	± 0.087	± 0.003	± 0.2	± 0.005	± 0.2	± 0.012
244	Sphere, rotation	± 0.123	± 0.006	± 0.2	± 0.010	± 0.2	± 0.010
4750	Fix planar target of 7 1”-RRs	± 0.962	± 0.018	± 0.2	± 0.013	± 0.2	± 0.024

III SUMMARY AND CONCLUSION

The available Elegant BB of the 3D Lidar for the Mars Sample Return mission fulfils nearly all performance requirements: It is able to acquire and track cooperative targets between 1 m and 5 km distance. Its 3 σ noise on range, azimuth and elevation (with the exceptions for the angular values at very short range mentioned above) is very low. A total mass of the future flight model below 7 kg is envisaged, based on an already achieved mass of the fully equipped sensor head of 1.6 kg only. FM power consumption will be in the order of 30 Watts.

The sensor concept, its technologies and design approach contains a lot of margin for sensor adaptation to several applications. Currently, we perform further development and upgrade of the RVS ILT BB in several projects founded by ESA and the German agency DLR.

Goals of these projects are on one hand qualification of major components of the 3D Lidar – Fibre laser, Gimbal mounted scanner, coaxial transmitter/ receiver optics – for application in future FMs. Over there, the transition to the large-sized 3D Lidar based on the technologies that were originally developed on the RVS ILT BB shall be performed. The large-size 3D Lidar of RVS ILT type is an excellent solution for servicing missions to non-cooperative satellites. Even the application of the scanning 3D Lidar for hazard avoidance and GNC support tasks during Landing missions is considered to be optimum, at least as long as the technologies for a 3D Lidar that is entirely scanner-free are not yet sufficiently advanced. In particular one advantage of the scanning 3D Lidar should be highlighted: Due to application of collimated transmitter / receiver beams these sensors are extremely robust against Sun impact on sensor and client side.

IV REFERENCES

[1] Statement of Work, Imaging Lidar Technology, Appendix 1, *ESA – AO/1-4794/05/NL/IA, 2005*

[2] Bettina Moebius, Karl-Hermann Kolk, Sigmund Manhart, “Development and Application of a Rendez-Vous and Docking Sensor RVS“, *Proceedings of “International Conference on Space Optics, 2-4 December 1997, Toulouse”*

[3] Tele-Goniometer Rendezvous Sensor - an Existing Sensor and its Growth Potential, B. Moebius, A. Ullrich, *Proceedings of the 24th International Symposium on Space Technology and Science, Miyazaki, Japan, 2004*

[4] Martin Pfennigbauer, Bettina Möbius, and João Pereira do Carmo, “Echo Digitizing Imaging LIDAR for Rendezvous and Docking”, in *Proc. SPIE Defense, Security & Sensing, Orlando, Vol. 7323, 732302-1 - 732302-9, April 2009.*

[5] Pfennigbauer, M., Möbius, B., Ullrich, A., do Carmo, J., “From long range to high precision – pushing the limits of pulsed-time-of-flight measurement”, *In Proc. SPIE Defense, Security & Sensing, Orlando, Vol. 7684, 768419, 2010.*

[6] Pfennigbauer, M., Ullrich, A., “Improving quality of laser scanning data acquisition through calibrated amplitude and pulse deviation measurement”, *In Proc. SPIE Defense, Security & Sensing, Orlando, Vol. 7684, 76841F, 2010.*

V ACKNOWLEDGEMENTS

Thank you very much to our colleagues at Jena-Optronik, RIEGL and ESTEC for their cooperation and support, for their excellent ideas and patience during technical consulting.

Vicariously for the colleagues at LusoSpace, sincere thanks are given to Carla Felix and Bruno Rodrigues for preparation and realization of the external longrange tests on RVS ILT.